Supplementary Information

Materials and Methods

Cell lines and plasmids: Cell lines were purchased from American Type Cell Culture (ATCC) and regularly tested for mycoplasma. MDA-MB-231-*fluc2-tdT* cells were engineered by stable transfection with pcDNA3.1(+)/Luc2-tdT (Addgene, #32904) and maintained under 400 µg/mL G418 selection.

Antibodies and reagents: Anti-pChk1 (Ser345) (133D3; #2348), anti-Chk1 (2G1D5; #2360), anti-pCDK1 (Tyr15) (10A11; #4539), anti-β-actin (13E5; #4970), anti-pHistone H2A.X (Ser139) (20E3; #9718), anti-Ki-67 (D3B5; #12202), anti-mouse IgG HRP-linked (#7076) and anti-rabbit IgG HRP-linked (#7074) were purchased from Cell Signalling, anti-pATR (Thr1989) (#GTX128145) from GeneTex. Immunoblotting was performed as previously described (1).

AZD6738 and AZD1775 were kindly provided by AstraZeneca. VE-821, ETP-46464, UCN-01 and Verapamil were purchased from Sigma.

Crystal violet assay: 5000 cells per well were seeded into 96 well plates 4 h prior to drug treatment. Cells were treated with indicated concentrations of AZD6738 (100 nM to 4000 nM) and AZD1775 (50 nM to 2000 nM) for 96 h. For siRNA treatment, cells were seeded into 96 well plates at a density of 4000 cells per well and cultured for 24 h prior to treatment. Cells were transfected with siRNA against Wee1 (Ambion; #s21) with 0.2% Lipofectamine RNAiMAX (ThemoFisher; #13778075) in multiples of 8 at the following final pM concentrations: 78.125, 156.25, 312.5, 625, 1250, 2500, 5000, 10000, and 20000, as well as no siRNA control. Transfected cells were then treated in quadruplicate with either AZD6738 (500 or 1000 nM) or vehicle (DMSO) for 96 h. After 96 h, cells were washed twice with 1X PBS and stained with 0.5% crystal violet (in 20% methanol) for 20 mins. Cells were then washed with water for 4 times, plates were air dried overnight. 200 µL methanol was added per well and incubated for 20 mins at room temperature. Optical density was measured at 584 nm using the FLUOstar Omega plate reader (BMG Labtech). Background values were subtracted using blank OD_{584}. Data was calculated in terms of % surviving attached cells (% crystal violet OD) compared to vehicle control treated cells. Experiments were performed in triplicates at least 3 times. To ensure that the Crystal Violet assay reflects cell survival, we compared some of the survival data measured by this method to cell survival observed by live cell imaging over the same period. We found that the two methods yielded very similar survival rates.

Cell synchronization and cell cycle analysis: U-2 OS cells were treated with 2 mM thymidine for 16 h, released into fresh medium for 4 h followed by nocodazole (100 ng/mL) treatment for 8 h. 6 h after release from nocodazole in to fresh medium, cells were treated with DMSO, AZD6738 (1 µM), AZD1775 (0.3 µM), or a combination of AZD6738 and AZD1775.

MDA-MB-231 cells were treated with 2 mM thymidine for 18 h, followed by release into fresh medium for 8 h and a second treatment with 2 mM thymidine for 18 h. After release, cells were treated with either DMSO, AZD6738 (1 µM), AZD1775 (0.3 µM), or combined AZD6738 and AZD1775.

For cell cycle analysis, cells were harvested at 2 h intervals and fixed with 70% chilled ethanol for at least 24 h at -20°C before a wash with 1X PBS. Pelleted cells (1500 rpm, 5 mins) were resuspended in

propidium iodide (PI) buffer (50 µg/mL) containing RNAse A (10 µg/mL) and incubated at 37°C for 30 mins. Samples were analyzed on a BD FACSCanto II flow cytometer.

Side population assay: Trypsinized MCF7 or MDA-MB-231 cells were counted using a hemocytometer. 1 x 10^6 cells were incubated for 15 mins at 37°C with 50 µg/mL Verapamil, a membrane transport blocker, and used as a negative control for gating. After 15 mins, cells in the negative control tube and the sample tube were stained with 0.5 µL DyeCycle Violet (DCV) dye (Thermofisher, USA) per million cells and incubated at 37°C for 90 mins with intermittent shaking. Cells were washed twice with 1X PBS (1500 rpm, 5 mins) and resuspended in sorting buffer. Samples were sorted using a BD FACSAria III flow cytometer.

Mammosphere assay: 1000 MCF7 and MDA-MB-231 side population (SP) and non-side population (NSP) sorted cells were seeded on 24-well ultra-low attachment plates (Corning, USA) in serum free DMEM/F12 medium containing a cocktail of EGF (10 ng/mL), Insulin (20 ng/mL), Lif1 (10 ng/mL; all from Sigma), and basic human FGF (20 ng/mL; Goldbio),). Medium was replenished every 3 days and mammospheres were cultured for 3 passages. Mammospheres were imaged at 10X magnification using a Zeiss Axiovert 200M inverted microscope (Carl Zeiss, Germany). Total number of mammospheres were counted under a light microscope.

For limited dilution (LD50) assays, SP/NSP sorted MCF7 and MDA-MB-231 cells were seeded in increasing concentrations (1, 2, 5, 10, 100, and 1000 cells/well) on 24-well ultra-low attachment plates in serum free media as described above. Wells were examined for mammospheres after 10 days under a light microscope and the observations were recorded as the number of wells containing mammospheres for each cell concentration.

Immunofluorescence: Cells were seeded on coverslips and synchronized using a double thymidine block. Released synchronized cells were treated with either vehicle, 1 µM AZD6738, 0.3 µM AZD1775, or a combination of AZD6738 and AZD1775 for 4 h and fixed with 4% paraformaldehyde (Sigma, USA) for 10 minutes at 37°C. Cells were then permeabilized in 4% paraformaldehyde with 0.2% Triton X-100 (Fisher Scientific, USA) for 10 minutes and blocked with 2% BSA for 30 minutes at room temperature. Cells were incubated with anti-centromere (ACA sera were kind gifts from Dr. M. Fritzler, University of Calgary, Calgary, Alberta, Canada) and anti-tubulin (Sigma; #T5168) antibodies at 37°C for 1 h each. Cells were washed with PBS and incubated with the dye-conjugated antibodies anti-human Alexa Fluor 647 and anti-rat Alexa Fluor 488 (Thermofisher, USA). Nuclei were counterstained with DAPI (5 µg/mL). Coverslips were mounted using the VECTASHIELD mounting medium for fluorescence (Vector Laboratories Inc., CA). Images were captured at 63X magnification using a Zeiss LSM 710 Meta Confocal Microscope (Carl Zeiss, Germany).

Live cell imaging: For analysis of mitotic timing, MDA-MB-231 stably expressing mCherry-H2B and GFP-Tubulin (2) were seeded in a 35 mm glass bottom dish (MatTek Corporation) and treated with vehicle, AZD6738, AZD1775, or combined AZD6738 and AZD1775. Plates were placed on a motor-controlled stage within an incubator chamber maintained at 37°C and 5% CO_2. Images were acquired using a spinning disc confocal inverted microscope (Axiovert 200M; Carl Zeiss) using the 40X objective lens and captured at 5 mins interval for 24 h (using the Volocity software). Movie files were exported as OME-TIFF files and further processed in Imaris 9.0.1 for background subtraction and noise reduction.

High-content screening microscopy: Images were taken with a High-content automated microscopy imaging system (MetaXpress Micro XLS, software version 6, Molecular Devices, Sunnyvale, CA, USA). Briefly, MDA-MB-231 cells were seeded onto a 96 well plate at a density of 4000 cells per well. Single images were captured in each well with a 20× (NA 0.75) objective equipped siCMOS camera using bandpass filters of 624/40 nm for mCherry. On average 200 cells images per well were manually analyzed with the MetaXpress software using mCherry-H2B to identify changes in DNA organization. Mitotic timing was calculated as the interval between nuclear envelope break down (NEBD, indicated by the first evidence of chromosome condensation) to the onset of anaphase (or chromosome decondensation in the case of mitotic slippage). The fates of cells (and resulting daughter cells) were tracked for the duration of the experiment (48 h). Cell death was determined by the formation of apoptotic bodies, loss of cell attachment, and/or loss of membrane integrity.

Assessment of mouse hematopoietic progenitor cells: 6 to 8 weeks old C57BL/6 mice were treated with inhibitors as described above for 26 days (n = 3 per group). Body weight was measured every 4 days as an indicator of toxicity. On the 27^{th} day, mice were euthanized by CO_2 asphyxiation and bone marrow was isolated from the femur by centrifugation at 14,000 rpm for 15 secs. Isolated bone marrow cells were resuspended in FACS buffer (1X PBS + 1% FBS) and cells were counted using a hemocytometer. 1×10^6 cells were stained with either PE anti-mouse CD117 (c-Kit) antibody (#105807) and/or Pacific Blue anti-mouse Lineage Cocktail (#133310) and/or FITC anti-mouse Ly-6A/E (Sca1) antibody (#108105) or PE rat IgG2b isotype (#400608) or Pacific Blue rat IgG2a isotype (#400527) or FITC rat IgG2a isotype (#400505; all from Biolegend) controls. Samples were analyzed on a BD FACSCanto II flow cytometer.

Immunohistochemistry: Immunohistochemistry was performed on formalin fixed paraffin embedded (FFPE) tissue samples using standard procedures as previously described (3). Briefly, 4 µm slices were sectioned on precleaned Colorfrost Plus microscope slides (Fisher Scientific, USA) using a microtome (Leica, Germany). Tissue samples were baked at 60°C for 2 h and deparaffinized 3 times in xylene for 10 mins each and subsequently rehydrated in a gradient of ethanol washes. Tissue sections were subjected to antigen retrieval in a pressure cooker using 0.05% citraconic anhydride antigen retrieval buffer (pH – 7.4). Tissue samples were blocked with 4% BSA for 30 mins and incubated with respective primary antibodies overnight at 4°C. Next day, endogenous peroxidase activity was blocked for 30 mins using 3% H_2O_2, followed by incubation with anti-rabbit HRP labelled secondary antibody (Dako EnVision+ System; K4007) for 1 h at room temperature in the dark. Samples were incubated with DAB (3,3'-diaminobenzidine) + substrate chromogen (Dako, USA) for brown color development, counter stained with hematoxylin, and mounted with DPX mounting medium (Sigma, USA). Images were captured using the Zeiss Axioskop2 plus upright microscope (Zeiss, Germany) equipped with AxioCam color camera (images on Figure 4 and 5), later upgraded to Axiocam 512 color camera (images on Figure 6, Suppl. Figure 7, 9, 10, and 11). Villi length (3 mice / treatment group) was measured using Fiji software (4).

TUNEL assay: TUNEL assay was performed for apoptosis detection using DeadEnd Fluorometric TUNEL System kit (G3250, Promega, USA) as per manufacturers instructions. Briefly, 4 µm slices were sectioned on precleaned Colorfrost Plus microscope slides (Fisher Scientific, USA) using a microtome (Leica, Germany). Samples were baked at 60°C for 2 h and deparaffinized by washing 2 times in xylene for 5 mins each and subsequently rehydrated in a gradient of ethanol washes followed by washing in 0.85% NaCl and 1x PBS solutions. Samples were then fixed with 4% methanol free formaldehyde for 15

mins and permeabilized with Proteinase K solution (20 μg/mL) at room temperature for 8 minutes. Samples were washed with PBS and fixed again with methanol-free formaldehyde solution. Samples were then allowed to equilibrate at room temperature using equilibration buffer. For labelling purposes, TdT reaction mix was added to the tissue area and covered with plastic coverslips to allow equal distribution. Samples were incubated for 60 mins at 37°C in a dark humidified chamber. Reaction was stopped by immersing slides in 2x SSC for 15 minutes. Tissue sections were counter stained with DAPI (5 μg/mL) and mounted using the VECTASHIELD mounting medium for fluorescence (Vector Laboratories Inc., CA). Images were captured at 40X magnification using a Zeiss LSM 710 Meta Confocal Microscope (Carl Zeiss, Germany).

Bioluminescence imaging: *In vivo* bioluminescence imaging was carried out as previously described (5). Briefly, mice were imaged using the Bruker In-Vivo Xtreme after intraperitoneal injection of D-Luciferin (3 mg/mouse). *Ex vivo* bioluminescence imaging was performed on major organs by immersing them in the D-Luciferin substrate. Sequential scans were acquired to capture the maximum kinetics of the luciferase reaction. Images of the luciferase scans were overlaid on the X-ray images acquired in the background. The light output was quantified using the Bruker MI SE software. Pseudocolor bars represent photon flux captured by the CCD camera.

Statistical analysis: All statistical analysis was performed using GraphPad Prism 7 software (GraphPad Software, La Jolla, California, USA). All experiments were performed at least 3 times in triplicates or quadruplets. *P*-values were calculated using one-way ANOVA, two-way ANOVA, and Log-rank (Mantel-Cox) test. *P*-values of < 0.05 were considered significant, and *P*-values of < 0.001 were considered highly significant.

References

1. Gamper AM, Rofougaran R, Watkins SC, Greenberger JS, Beumer JH, Bakkenist CJ. ATR kinase activation in G1 phase facilitates the repair of ionizing radiation-induced DNA damage. Nucleic Acids Res **2013**;41(22):10334-44 doi 10.1093/nar/gkt833.
2. Moudgil DK, Westcott N, Famulski JK, Patel K, Macdonald D, Hang H, *et al.* A novel role of farnesylation in targeting a mitotic checkpoint protein, human Spindly, to kinetochores. J Cell Biol **2015**;208(7):881-96 doi 10.1083/jcb.201412085.
3. Varghese F, Bukhari AB, Malhotra R, De A. IHC Profiler: an open source plugin for the quantitative evaluation and automated scoring of immunohistochemistry images of human tissue samples. PLoS One **2014**;9(5):e96801 doi 10.1371/journal.pone.0096801.
4. Schindelin J, Arganda-Carreras I, Frise E, Kaynig V, Longair M, Pietzsch T, *et al.* Fiji: an open-source platform for biological-image analysis. Nat Methods **2012**;9(7):676-82 doi 10.1038/nmeth.2019.
5. Rengan AK, Bukhari AB, Pradhan A, Malhotra R, Banerjee R, Srivastava R, *et al.* In vivo analysis of biodegradable liposome gold nanoparticles as efficient agents for photothermal therapy of cancer. Nano Lett **2015**;15(2):842-8 doi 10.1021/nl5045378.

Supplementary Figures

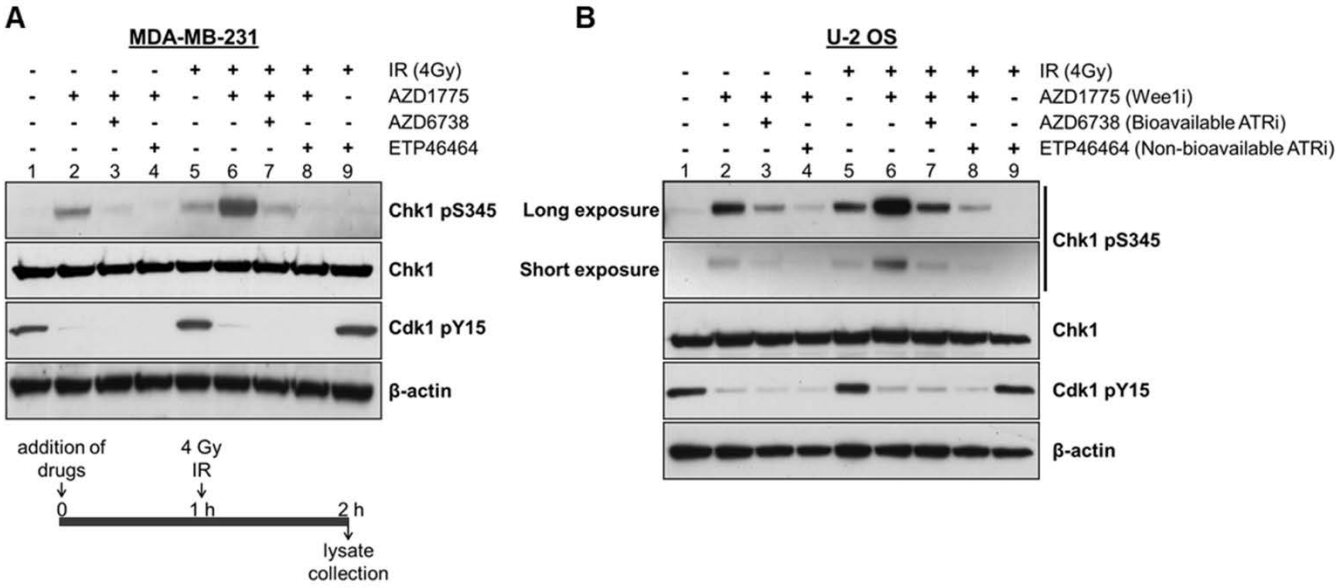

Supplementary Figure 1. Wee1 inhibition activates ATR. MDA-MB-231 **(A)** and U2OS **(B)** cells where incubated with the indicated inhibitors. After 1 hour cells were irradiated with 4 Gy or mock treated. After another hour cell lysates were harvested and probed for Chk1 and CDK1 phosphorylation by immunoblotting. Inhibition of Wee1 by AZD1775 leads to activation of ATR (see decrease in phospho-CDK1 levels and increase in phospho-Chk1 in lane 2). AZD6738 and ETP46464 are selective ATR inhibitors. DNA damaging agents such as ionizing radiation (IR) can combine with Wee1 inhibition in activating ATR. Figure 1A is a subset of this figure derived from the same experiment.

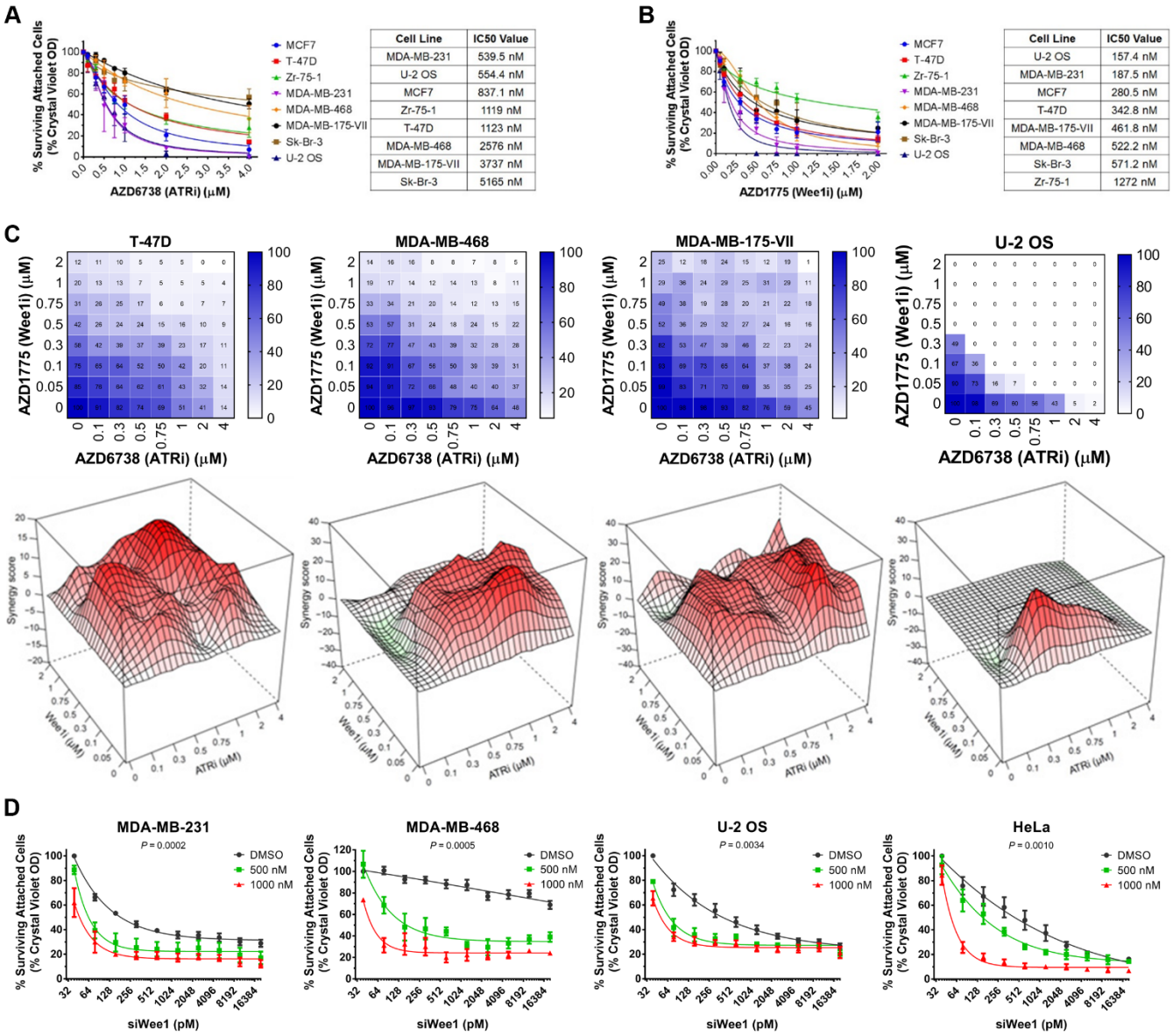

Cell Line	IC50 Value
MDA-MB-231	539.5 nM
U-2 OS	554.4 nM
MCF7	837.1 nM
Zr-75-1	1119 nM
T-47D	1123 nM
MDA-MB-468	2576 nM
MDA-MB-175-VII	3737 nM
Sk-Br-3	5165 nM

Cell Line	IC50 Value
U-2 OS	157.4 nM
MDA-MB-231	187.5 nM
MCF7	280.5 nM
T-47D	342.8 nM
MDA-MB-175-VII	461.8 nM
MDA-MB-468	522.2 nM
Sk-Br-3	571.2 nM
Zr-75-1	1272 nM

Supplementary Figure 2. Wee1 and ATR inhibition synergistically kills cancer cells. (A) IC_{50} values for AZD6738 in cancer cells. Cells were treated for 4 days with up to 4 μM AZD6738 and survival was assayed by Crystal Violet staining. **(B)** IC_{50} values for AZD1775 in cancer cells. Four day survival relative to control was measured like in (A). **(C)** Synergistic killing of cancer cells by AZD6738 and AZD1775. Cooperative cell killing was measured by treating cells with the indicated drug concentrations or vehicle control. Color bars indicate % survival normalized to vehicle treated cells. Representative cooperativity screens and Loewe plots for drug cooperativity are shown. Bliss combination indices (CI) at indicated drug concentrations are shown in Table 1. **(D)** Cooperative cell killing by Wee1 knockdown and ATR inhibition. Control or cells treated with AZD6738 at indicated concentrations were transfected with increasing doses of siRNA against Wee1 and assayed for viability after 4 days by Crystal Violet staining as described (Lewis et al., Oncotarget 2017). Statistical analysis was performed using 2way ANOVA.

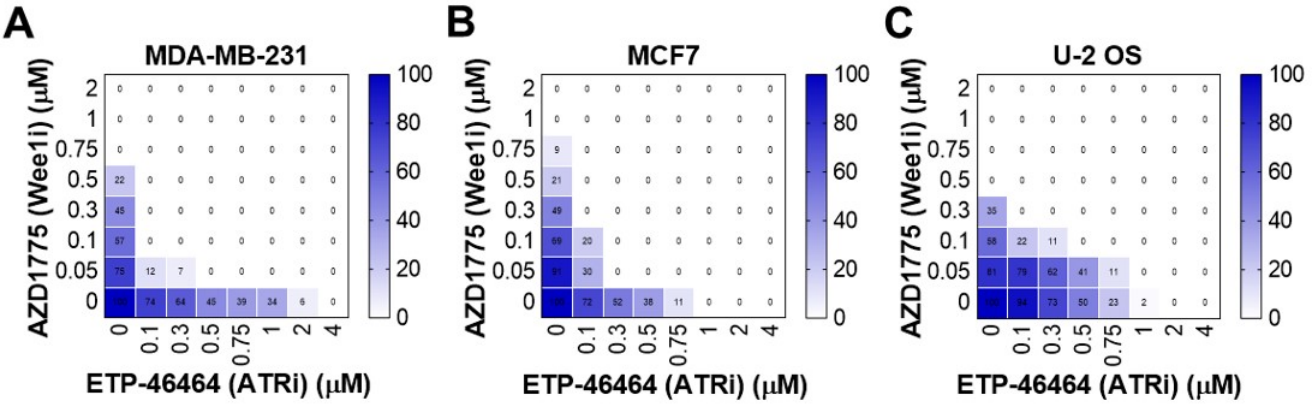

D

Cell Line	ETP-46464 (ATRi)	AZD1775 (Wee1i)	Bliss CI	ATRi IC_{50}	Wee1i IC_{50}
MDA-MB-231	100 nM	50 nM	0.50	431 nM	190 nM
MCF7	100 nM	50 nM	0.49	265 nM	280 nM
U-2 OS	100 nM	100 nM	0.58	463 nM	160 nM

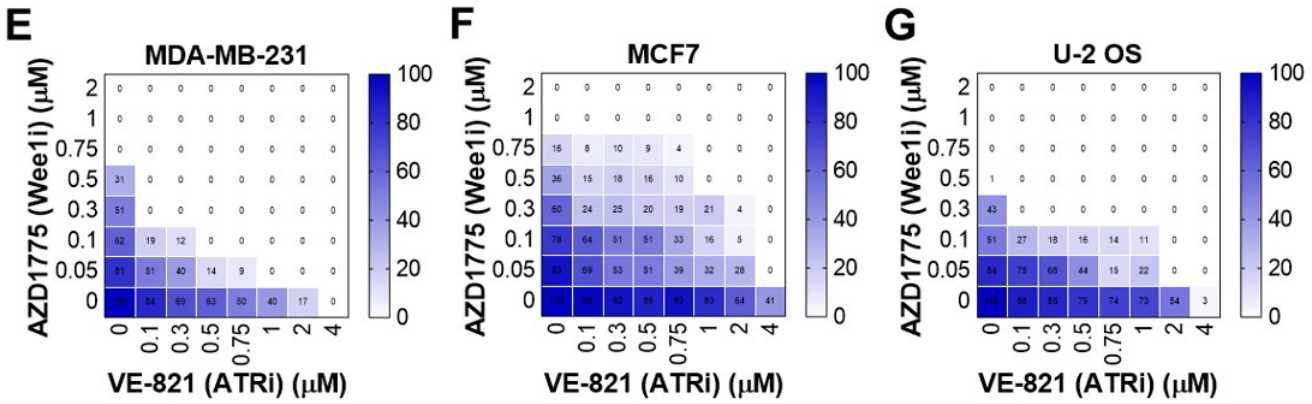

H

Cell Line	VE-821 (ATRi)	AZD1775 (Wee1i)	Bliss CI	ATRi IC_{50}	Wee1i IC_{50}
MDA-MB-231	100 nM	100 nM	0.59	662 nM	190 nM
MCF7	100 nM	50 nM	0.28	3124 nM	280 nM
U-2 OS	100 nM	300 nM	0.62	1585 nM	160 nM

Supplementary Figure 3. Wee1 and ATR inhibition synergistically kills cancer cells. (A-C) Synergistic killing of cancer cells by ETP-46464 and AZD1775. Cooperative cell killing was measured by treating cells with the indicated drug concentrations or vehicle control. Color bars indicate % survival normalized to vehicle treated cells. **(D)** Table shows Bliss combination indices (CI) at indicated drug concentration. **(E-G)** Plots show synergistic killing of cancer cells by VE-821 and AZD1775. **(H)** Table shows Bliss CI at indicated drug concentrations.

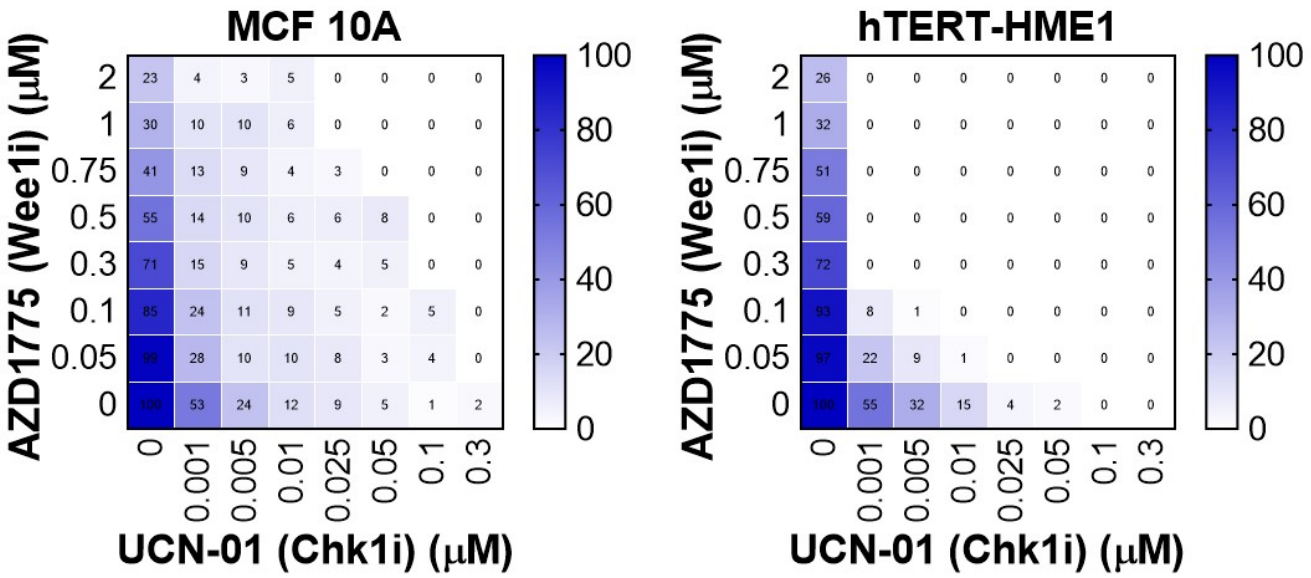

Supplementary Figure 4. The Chk1 inhibitor UCN-01 is highly toxic in MCF10A and hTERT-HME1, alone and in combination with AZD1775. Synergistic killing of "normal" cells by UCN-01 and AZD1775. Cooperative cell killing was measured by treating cells with the indicated drug concentrations or vehicle control. Color bars indicate % survival normalized to vehicle treated cells. Representative cooperativity screens are shown.

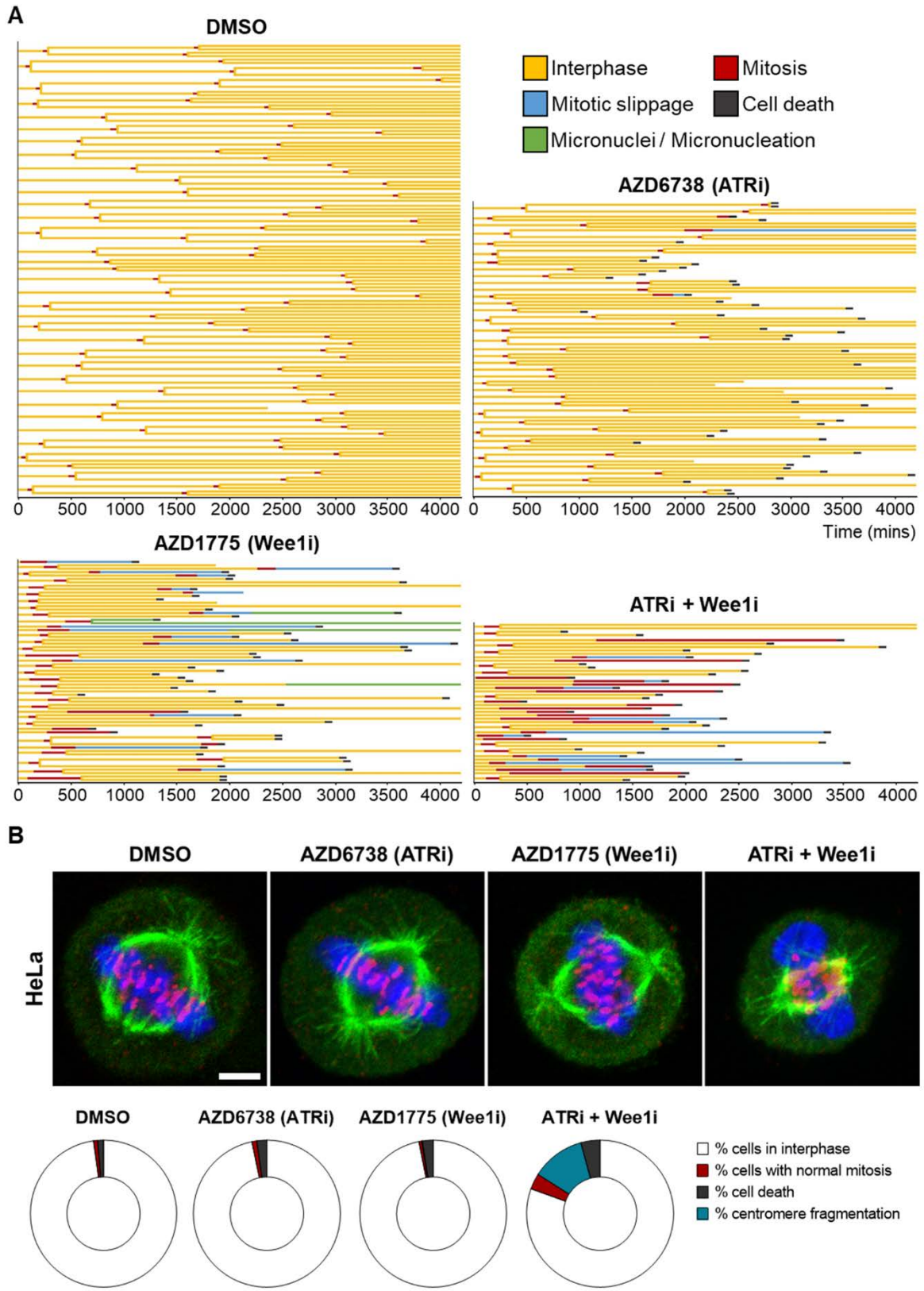

Supplementary Figure 5. Combined ATR and Wee1 inhibition leads to mitotic defects and cancer cell death. (A) Representative fates of MDA-MB-231 cells (n = 35) in the 4 treatment groups. **(B)**

Representative images of mitotic HeLa cells treated with ATR and/or Wee1 inhibitor (ATRi = 1 μM AZD6738, Wee1i = 0.3 μM AZD1775). Fixed cells were stained for centromeres (red) and tubulin (green) by immunofluorescence and for DNA with DAPI (blue). Drug-induced clustering of centromeres spatially separated from the main mass of chromosome, a feature of centromere fragmentation, is clearly visible. Quantification of cells (n > 1000), fixed 4 h after release from a double thymidine block in the presence of the indicated inhibitors, that are in mitosis (red and blue) and display centromere fragmentation (blue).

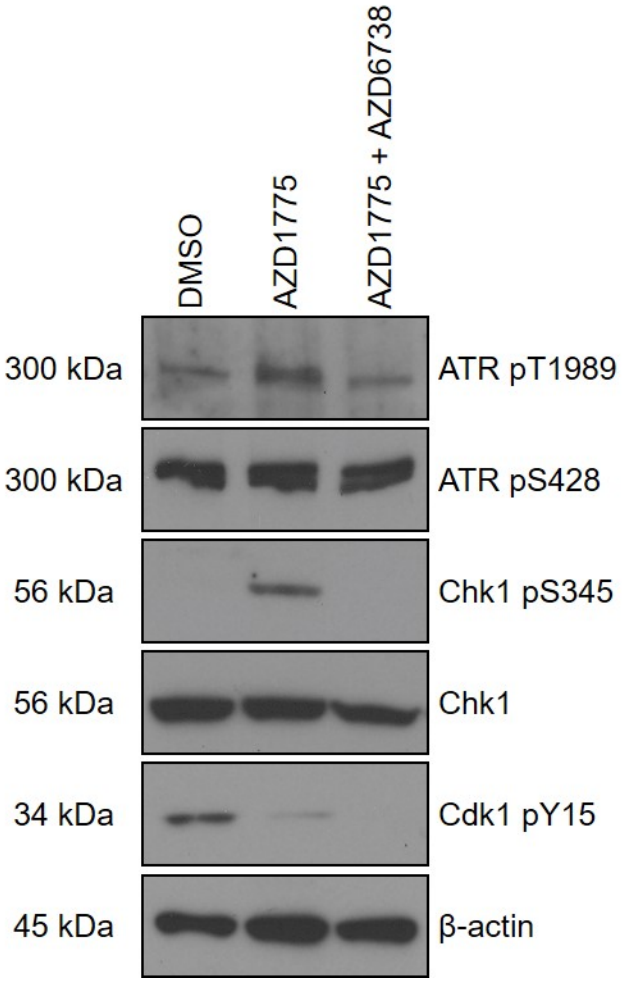

Supplementary Figure 6. MDA-MB-231 cells were treated for 24 h with AZD1775 (300 nM), AZD1775 combined with AZD6738 (1 µM), or vehicle control (DMSO) before harvesting and analysing their lysates by immunoblotting. Unlike phosphorylation of ATR at Serine 428, phosphorylation at Threonine 1989 correlates with the phosphorylation of Chk1 at Serine 345, indicating that the phosphorylation status of ATR T1989 can be used as biomarker for ATR activation in agreement with Nam et al. (J. Biol. Chem. 2011).

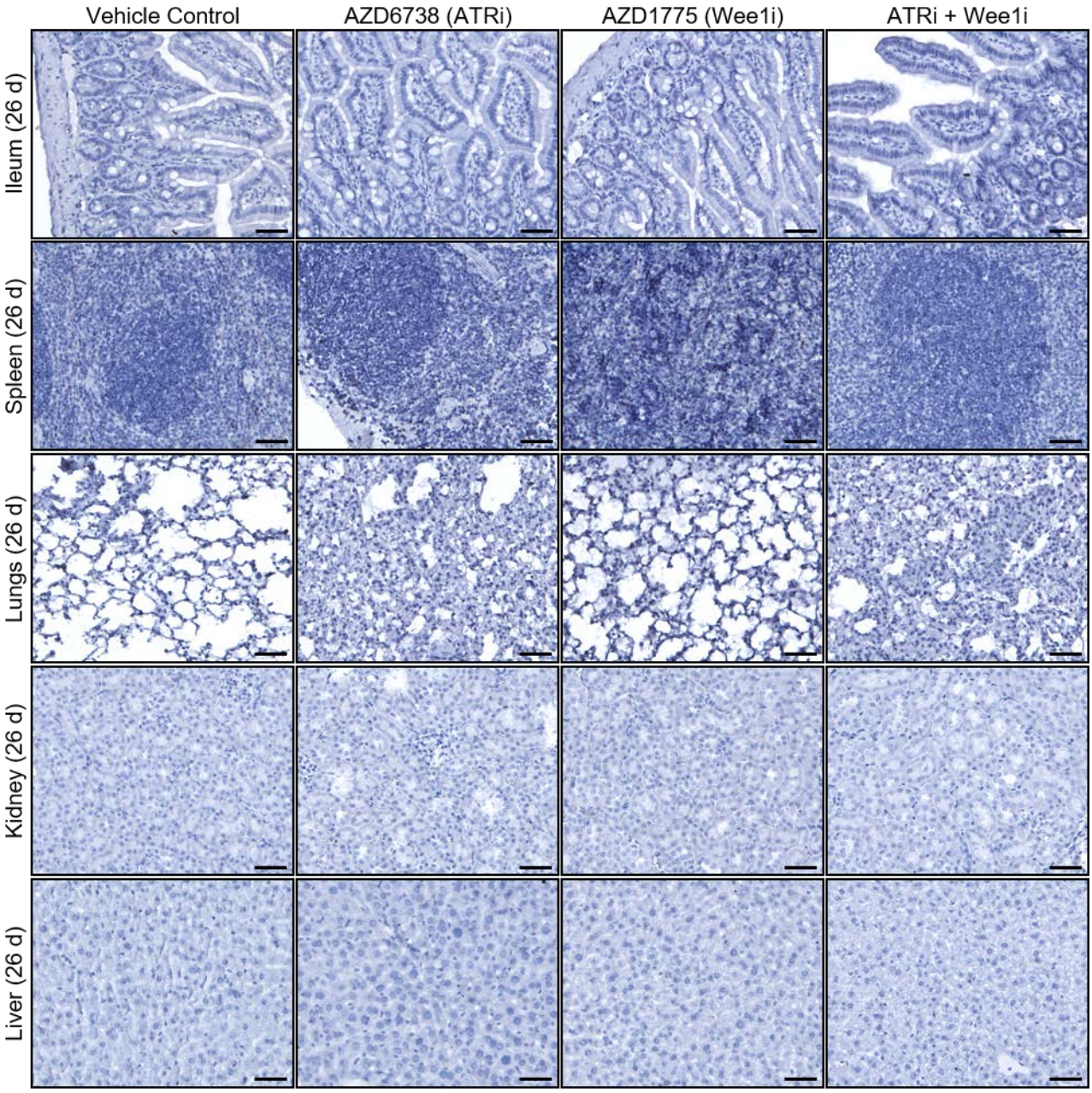

Supplementary Figure 7. Immunohistochemistry evaluation of ATR pThr1989 levels in normal tissues of NSG mice 26 days post treatment with ATR and/or Wee1 inhibitors. Scale = 25 μm.

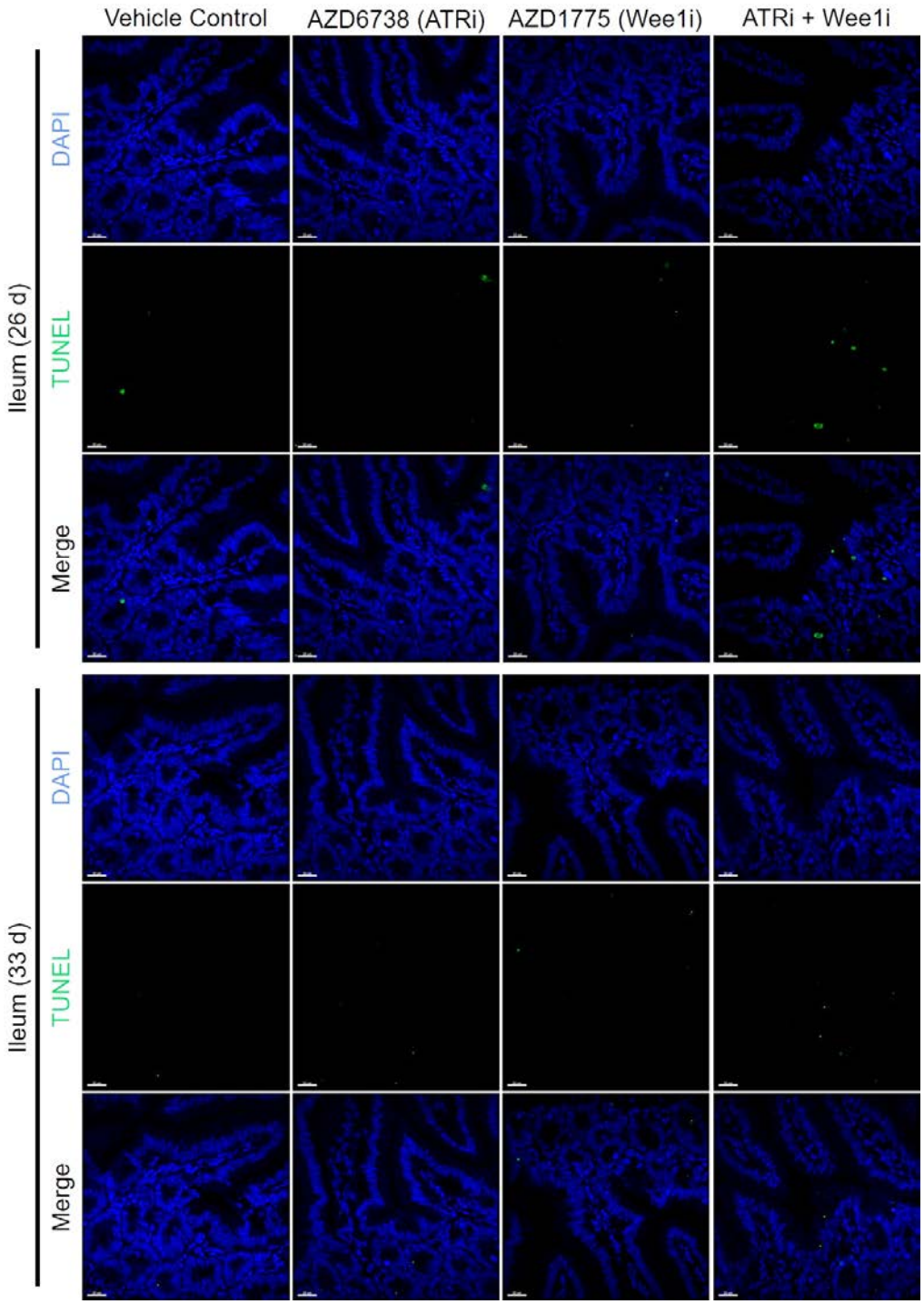

Supplementary Figure 8. Evaluation of apoptotic cells by TUNEL assay in ileum at 26- and 33-day time points post treatment with ATR and/or Wee1 inhibitors. Scale = 20 μm.

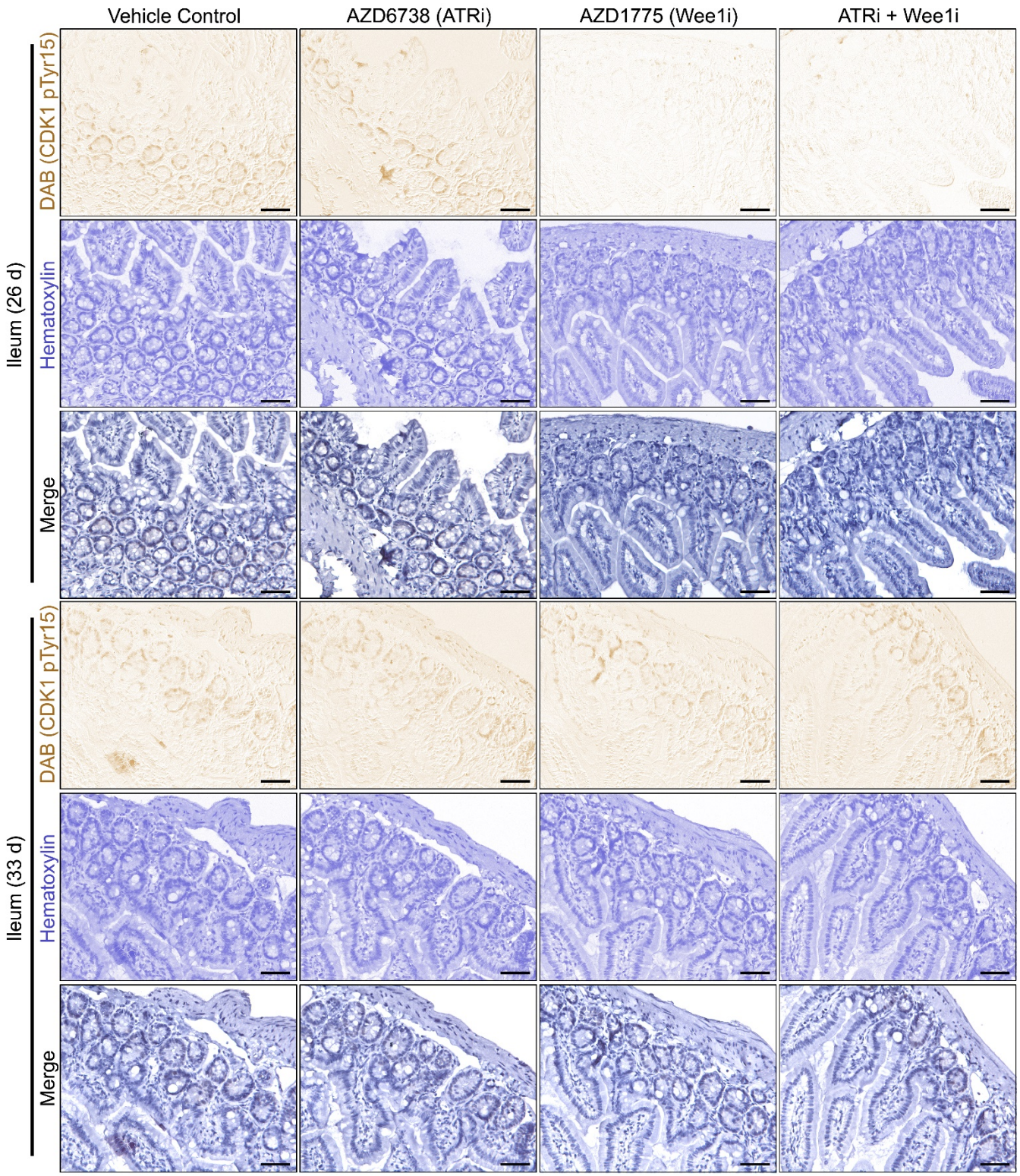

Supplementary Figure 9. Immunohistochemistry evaluation of CDK1 pTyr15 levels in Ileum of NSG mice at 26- and 33-days post treatment with ATR and/or Wee1 inhibitors. Scale = 25 μm.

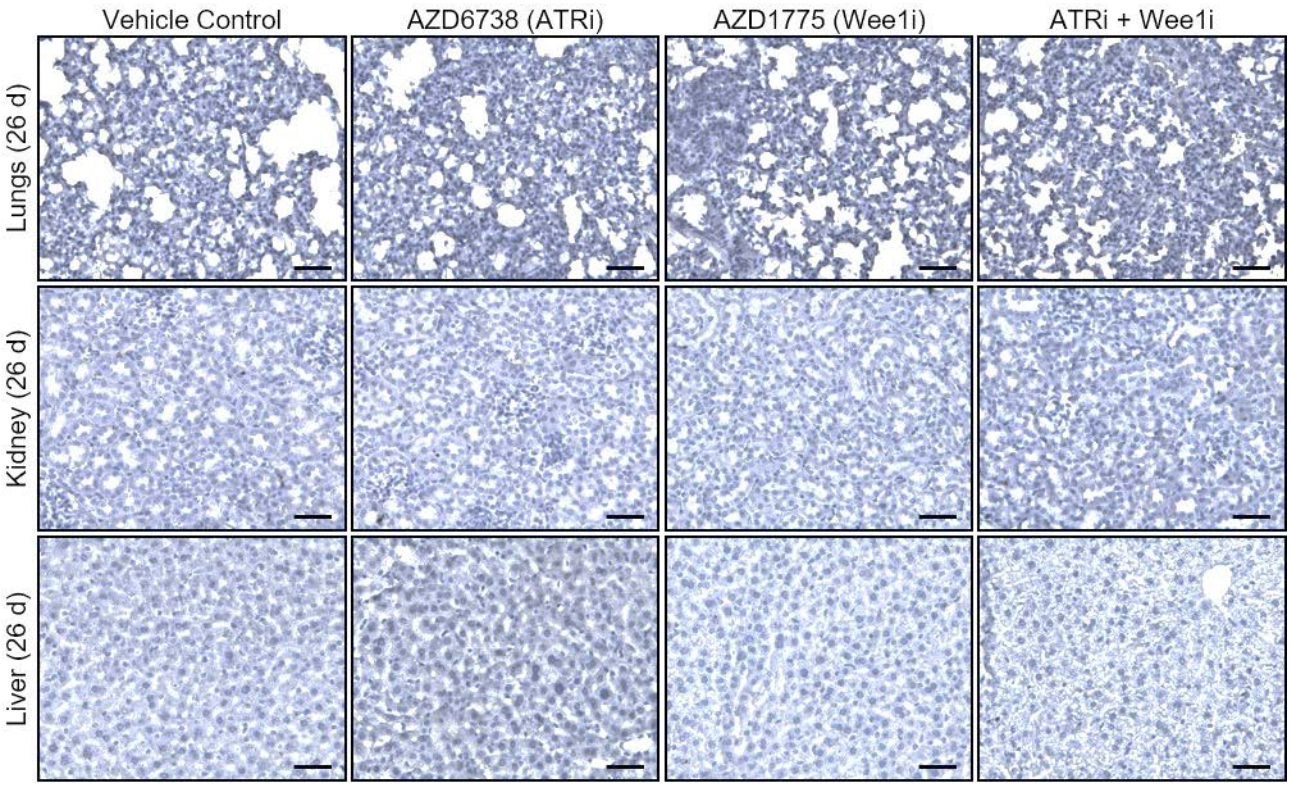

Supplementary Figure 10. Immunohistochemistry evaluation of CDK1 pTyr15 in normal tissue of NSG mice 26 days post treatment with ATR and/or Wee1 inhibitors. Scale = 25 μm.

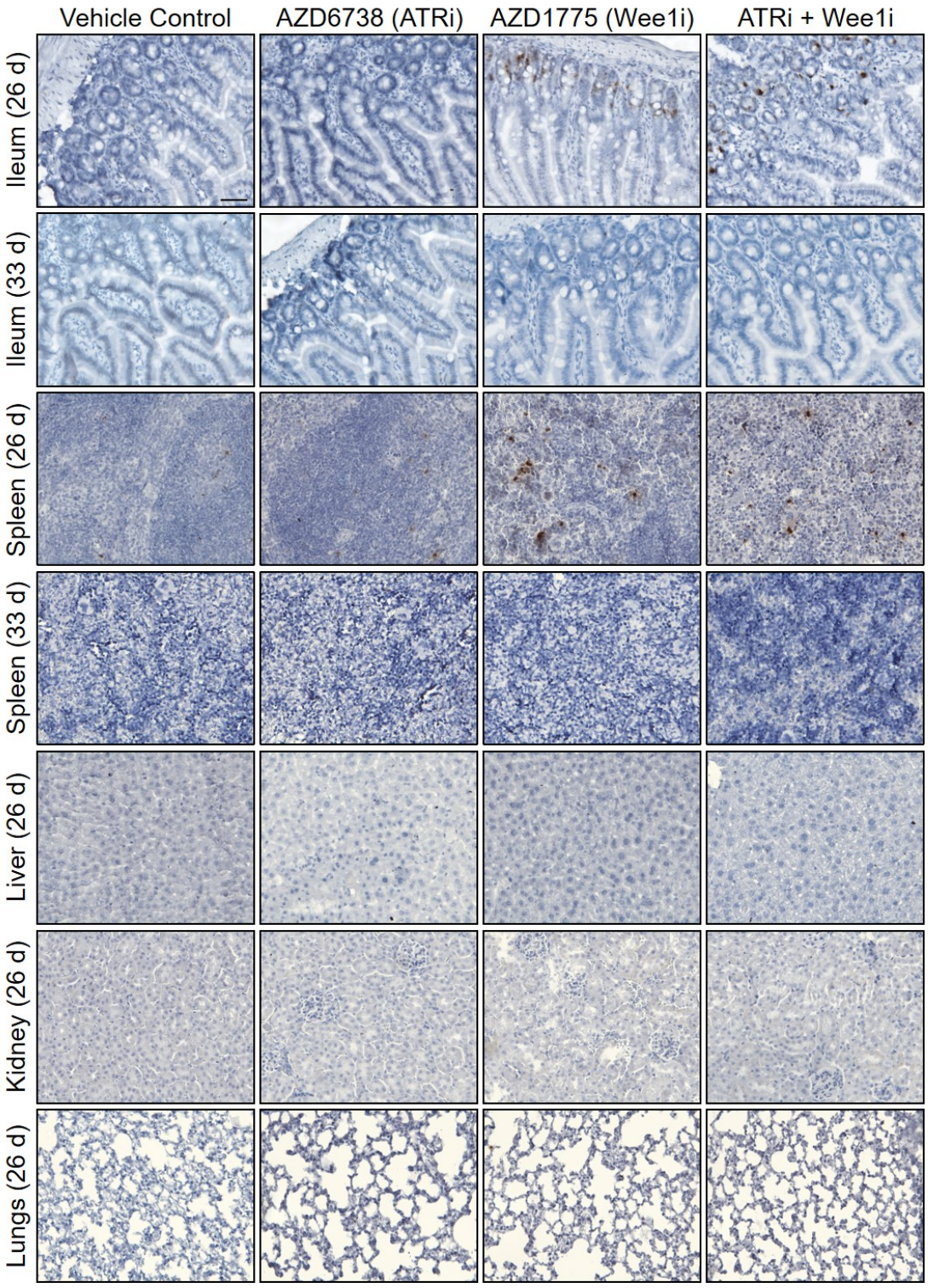

Supplementary Figure 11. Immunohistochemistry evaluation of γH2AX staining in normal tissue of C57BL/6 mice 26 days post treatment with ATR and/or Wee1 inhibitors. Scale = 25 μm.

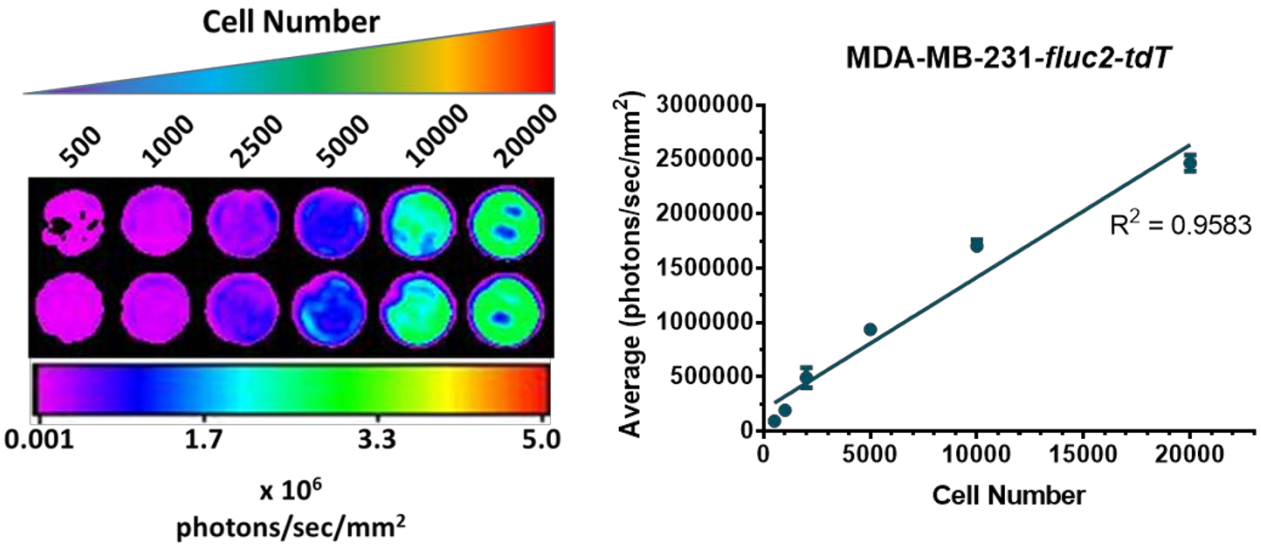

Supplementary Figure 12. Quantification of photon flux for MDA-MB-231-*fluc2-tdTomato* cells in vitro. Increasing numbers of cells were plated, D-luciferin was added, and images were taken using the Bruker In-Vivo Xtreme optical imager to measure linearity of the signal.

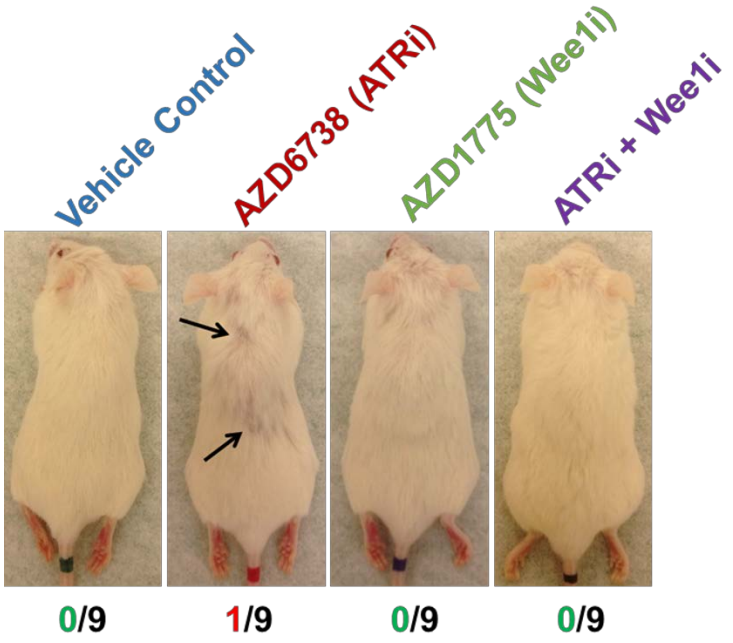

Supplementary Figure 13. Hair growth changes in mice treated with ATR and/or Wee1 inhibitors. Tumor-bearing NSG mice were randomly assigned to treatment groups and treated for 26 days with 25 mg/kg AZD6738 and/or 60 mg/kg AZD1775 daily for longitudinal studies as described in Figure 6 A-E. Only one mouse (depicted) showed signs of partial hair loss.

None of the NSG mice (n = 4 per cohort) used for experiments described in Figure 6F-H or C57BL/6 mice used in experiments described in Figure 5C showed any signs of hair loss, despite being treated 26 days with 25 mg/kg AZD6738 and/or 60 mg/kg AZD1775 per diem.

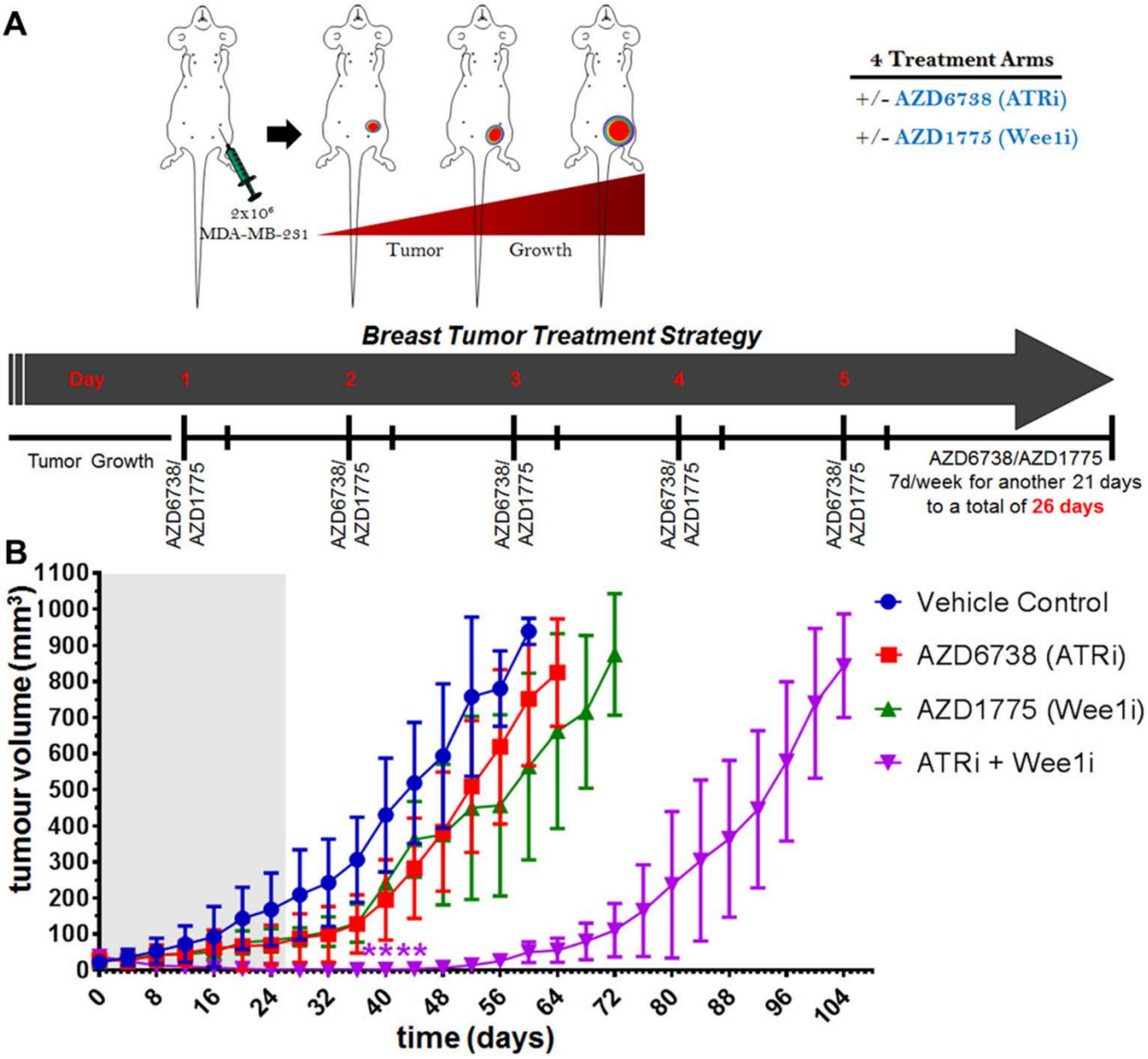

Supplementary Figure 14. Longitudinal studies of tumor-bearing mice treated with ATR and Wee1 inhibitors. (A) Treatment plan. NSG mice were injected with MDA-MB-231-*fluc2-tdTomato* labelled breast cancer cells in an orthotopic xenograft mouse model, randomly assigned to treatment groups when tumors reached 40-50 mm^3, and treated for 26 days with 25 mg/kg AZD6738 and/or 60 mg/kg AZD1775. **(B)** Tumor growth of mice in the four treatment arms (n = 9). The shaded area indicates duration of the treatment.

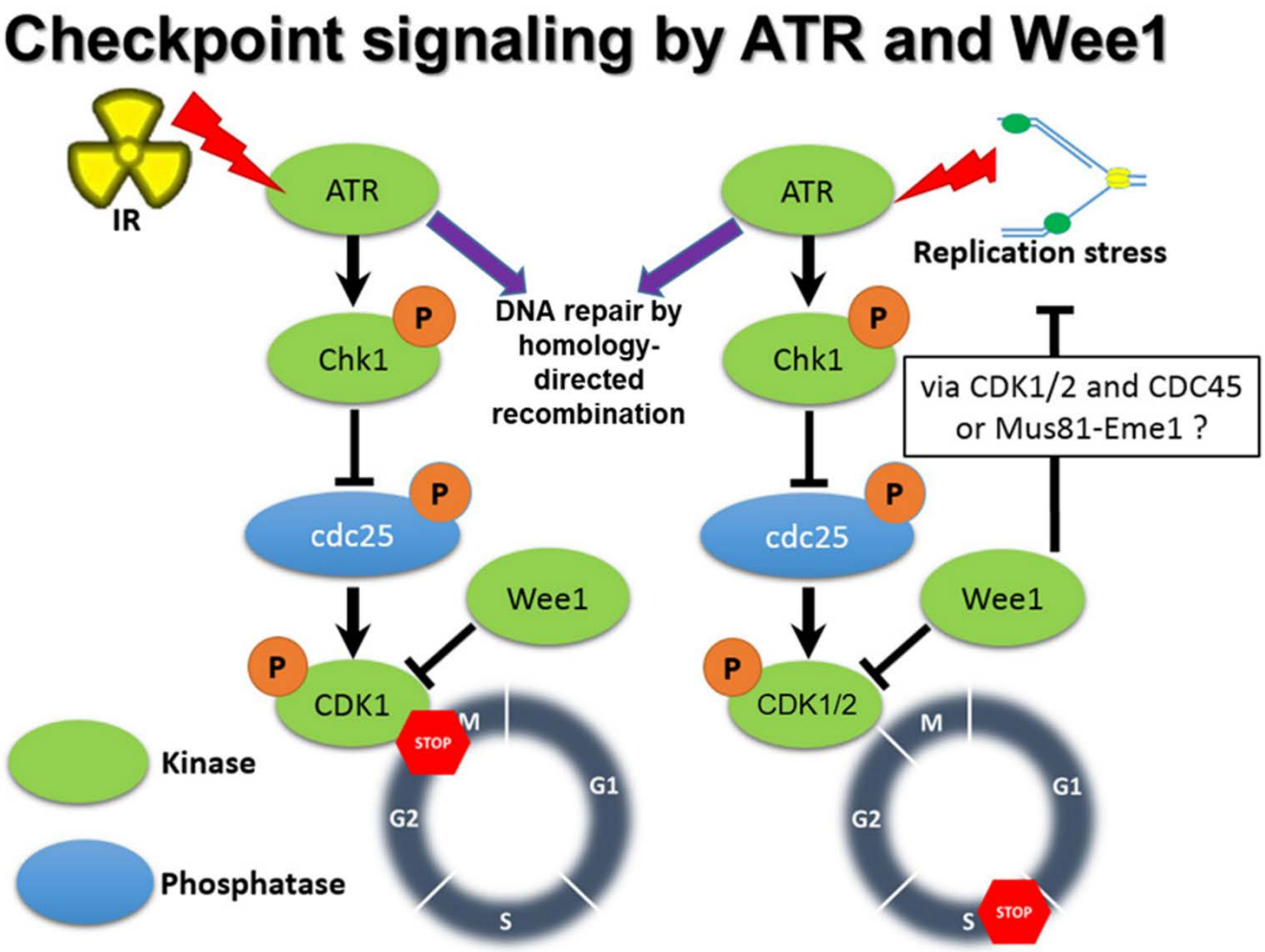

Supplementary Figure 15. G2/M and S phase checkpoint regulation by ATR and Wee1. The activity of the cyclin-dependent kinases CDK1 and CDK2 regulates the G2/M and S phase cell cycle checkpoints. Besides by binding to the appropriate cyclins (not shown), the activity of these CDKs is regulated by their phosphorylation state, which in turn is determined by the protein kinase Wee1 and the counter-acting protein phosphatase cdc25.

Activation of ATR by RPA-coated single-stranded DNA, structures resulting from replication fork uncoupling or resection of DNA double strand breaks (e.g. after ionizing radiation), leads to activating phosphorylation of Chk1 at serines 317 and 345. Chk1 in turn phosphorylates cdc25 leading to cdc25 inhibition and targeting for degradation. ATR activation thus leads to increased phosphorylation and inhibition of CDK1/2. Of note, Wee1 inhibition was reported to increase replication stress, by a still poorly understood mechanism.

ATR also positively regulates homology-directed recombination, an important DNA repair mechanism during S and G2 phase.

HEMATOLOGY									
Sample ID	**WBC ($x10^9$/L)**	**RBC ($x10^{12}$/L)**	**Hemoglobin (g/L)**	**Hematocrit (L/L)**	**MCV (fl)**	**MCH (pg)**	**MCHC (g/L)**	**RDW (%CV)**	**Platelets ($x10^9$/L)**
Vehicle Control (26 d)	2.55±0.6	10.75±0.6	167±12	0.48±0.01	44.45±1.4	15.5±0.28	349±18	22.7±2.1	904±370
Vehicle Control (33 d)	4.6±1.13	10.75±0.63	167±12	0.48±0.01	44.45±1.48	15.5±0.28	325±2	21.85±0.07	817±540
Vehicle Control (40 d)	4.4±2.26	9.9±0.56	150±7	0.45±0.02	45.65±0.7	15.15±0.2	332±1	21.45±0.7	840±405
AZD6738 (ATRi) (26 d)	6.8±0.28	10.4±1.2	156±15	0.49±0.05	47.9±1.41	15±0.42	314±1	22.35±1.6	524±186
AZD6738 (ATRi) (33 d)	7.75±3.46	9.4±0.28	142±5	0.44±0.007	47.35±1.34	15±0.21	319±14	21±1.13	619±332
AZD6738 (ATRi) (40 d)	7.75±2.3	9.75±0.07	146±1	0.45±0.007	46.6±0.14	15±0.14	321±4	23.4±0.7	513±255
AZD1775 (Wee1i) (26 d)	7.05±2.2	10.6±0.56	160±4	0.51±0.03	48.6±0.7	15.2±0.42	313±13	22.5±0.7	670±190
AZD1775 (Wee1i) (33 d)	4.3±2.5	9.85±0.07	150±1	0.44±0.007	45.5±0.3	15.45±0.35	334±2	21.8±0.42	694±29
AZD1775 (Wee1i) (40 d)	9.4±0.7	10.25±0.63	157±12	0.48±0.03	47.2±0.2	15.3±0.28	324±7	22.75±1.06	763±394
ATRi + Wee1i (26 d)	5±2.4	10.3±0.14	162±2	0.48±0.01	46.15±1.2	15.6±0.14	338±12	22.35±0.07	778±423
ATRi + Wee1i (33 d)	8.6±2.7	10.25±0.63	160±11	0.5±0.03	48.9±0.56	15.65±0.21	319±7	22.1±0.14	1023±365
ATRi + Wee1i (40 d)	9.1±3.1	10.65±0.35	163±6	0.5±0.007	47.45±0.91	15.15±0.21	322±6	22.1±0.14	1085±566

Supplementary Table 1: Table represents complete blood count (CBC) analysis of C57BL/6 mice treated for 26 days with either vehicle control or AZD6738 (ATRi) or AZD1775 (Wee1i) or combined treatment of AZD6738 and AZD1775 (n = 3 per group). Whole blood samples were collected by cardiac puncture at day 26, 33, and 40. Pathological evaluation revealed no signs of abnormalities.

Sample ID	Neutrophils		Lymphocytes		Monocytes		Eosinophils		Basophils	
	%	abs	%	abs	%	abs	%	Abs	%	abs
Vehicle Control (26 d)	10±2.8	0.25± 0.07	87.5±5	2.2±0.6	2.5±2.1	0.3±0.2	0	0	0	0
Vehicle Control (33 d)	5.5±0.7	0.25± 0.07	87±7	3.9±0.6	6.5±4.9	0.3±0.2	1±1	0.05± 0.07	0	0
Vehicle Control (40 d)	15±11.3	0.8±0.8	77.5±13	3.2±1.2	7±2.8	0.3±0.2	0.3±0.5	0	0	0
AZD6738 (ATRi) (26 d)	8±4.2	0.5±0.3	83±2.8	5.6± 0.07	8±1.4	0.5± 0.07	1±0	0.1±0	0	0
AZD6738 (ATRi) (33 d)	8±2.1	0.6±0.4	86±1.4	6.6±2.9	5±2.1	0.4±0	1±0.3	0.1±0	0	0
AZD6738 (ATRi) (40 d)	14±4.2	1.2±0.6	81±2.1	6.3±1.7	4±1.4	0.3±0	1±0.3	0.1±0	0	0
AZD1775 (Wee1i) (26 d)	9.5±2.1	0.7±0.1	78.5±1	5.5±1.7	8.5±2.1	0.6±0	3.5±3	0.3±0.2	0	0
AZD1775 (Wee1i) (33 d)	8±1.4	0.4±0.2	81.5±4	3.5±1.9	6±0.7	0.3±0.1	4±1.4	0.2±0.1	0	0
AZD1775 (Wee1i) (40 d)	5.6±0.5	0.6±0.1	81±6	7.6±0.5	7.1±1.2	0.7±0.1	5.7±4.6	0.5±0.4	0	0
ATRi + Wee1i (26 d)	11±2.8	0.6±0.4	78±2.1	3.9±1.8	4±0.7	0.3±0.1	6±0	0.3±0.1	0	0
ATRi + Wee1i (33 d)	11±3.5	0.9±0.2	78±1.4	6.7±2.1	4±0	0.4±0.1	6±2	0.6±0.4	0	0
ATRi + Wee1i (40 d)	11±8.4	0.9±0.4	76±14.1	7.2±3.6	5±0	0.5±0.2	8±5.6	0.7±0.2	0	0

Supplementary Table 2. Table represents manual differential analysis of C57BL/6 mice treated for 26 days with either vehicle control or AZD6738 (ATRi) or AZD1775 (Wee1i) or combined treatment of AZD6738 and AZD1775 (n = 3 per group) performed by a pathologist at IDEXX laboratories. Whole blood samples were collected by cardiac puncture at day 26, 33, and 40. Pathological evaluation revealed no signs of abnormalities.